

Epidermal cells accelerate the restoration of the blood flow in diabetic ischemic limbs

Chunhua Jiao^{1,*}, Sarah Bronner^{2,*}, Keri L. N. Mercer^{2,*}, Don D. Sheriff¹, Gina C. Schatteman¹ and Martine Dunnwald^{2,‡}

¹Department of Exercise Science, ²Joe Marshall Laboratory, Department of Dermatology, The University of Iowa, Iowa City, IA 52242, USA

*These authors contributed equally to this work

‡Author for correspondence (e-mail: martine-dunnwald@uiowa.edu)

Accepted 7 October 2003

Journal of Cell Science 117, 1055-1063 Published by The Company of Biologists 2004
doi:10.1242/jcs.00926

Summary

Epidermal progenitor cells (EpPCs) were long thought to be unipotent, giving rise only to other keratinocytes but recent studies question this assumption. Here, we investigated whether mouse EpPCs can adopt other antigenic and functional phenotypes. To test this, we injected freshly isolated and cultured EpPCs and transient amplifying cells into diabetic and non-diabetic mouse ischemic hindlimb and followed the cells' fate and the recovery of the ischemic limb blood flow over time. Both freshly isolated and cultured EpPCs and transient amplifying cells were incorporated into the vasculature of the ischemic limb 2 and 5 weeks post-injection, and some expressed endothelial cell but not keratinocyte antigens. Additionally, in the non-diabetic animals, first transient amplifying cells and then EpPCs accelerated the restoration of the blood flow. By contrast, in diabetic

animals, only injected EpPCs or unsorted epidermal cells accelerated the restoration of the blood flow. These data indicate that epidermal cells can adopt non-skin phenotypes and functions, and that this apparent pluripotency is not lost by differentiation of EpPCs into transient amplifying cells. They also suggest that epidermal cell therapy might be of therapeutic value in the treatment of diabetic ischemia. Finally, because epidermal cells are readily accessible and expandable, they appear to be ideally suited for use as a non-viral gene delivery therapy.

Movies available online

Key words: Epidermal progenitor cells, Vascularization, Epidermis, Ischemia, Plasticity

Introduction

The epidermis, the outermost layer of the skin, is a stratified cornified epithelium maintained by division of small undifferentiated stem and progenitor cells in the proliferative basal layer that replace cells in the stratum corneum that is shed into the environment. These undifferentiated cells divide infrequently but, when they proceed through the cell cycle, they give rise to both another undifferentiated cell and a progeny, called a transient amplifying (TA) cell (Hall and Watt, 1989; Potten and Loeffler, 1990). TA cells divide rapidly and terminally differentiate into corneocytes (Bickenbach and Dunnwald, 2000). Many fundamental questions related to epidermal stem-cell biology, including their potential plasticity, remain largely unanswered because of the lack of specific markers. We took a different approach and modified a previously published method for isolating hematopoietic stem cells (Goodell et al., 1996), allowing us to sort mouse epidermal cells into two populations: the progenitor cells and the more differentiated TA cells.

Until recently, epidermal stem cells and hair-follicle stem cells were thought to be unipotent, giving rise only to other keratinocytes, consistent with the conventional wisdom that the lineage potential of adult stem cells is restricted to the tissue of origin. This notion has been challenged by recent findings that epidermal stem cells generate cells from different lineages when injected into blastocysts and that hair-follicle stem cells

are precursors of epidermal cells as well as cells from the sebaceous gland (Liang and Bickenbach, 2002; Oshima et al., 2001; Taylor et al., 2000).

A much broader plasticity has been attributed to bone-marrow stem cells. After injection in an irradiated host, they can form astroglia and microglia in the brain, skeletal muscle cells, and new hepatic oval cells (Eglitis and Mezey, 1997; Ferrari et al., 1998; Petersen et al., 1999). Hematopoietic stem cells contribute to epithelial tissues, liver cells and cardiac myocytes, and were also found in the brain (Gussoni et al., 1999; Jackson et al., 2001; Kopen et al., 1999; Krause et al., 2001; Lagasse et al., 2000; Mezey et al., 2000; Orlic et al., 2001; Theise et al., 2000a). More surprising, dermal cells express markers of neurons, glia, smooth muscle cells and adipocytes when grown in defined culture conditions (Toma et al., 2001). Using a mouse model of unilateral hindlimb ischemia, several groups have shown not only that the blood contains endothelial cell progenitors (Asahara et al., 1997) but also that these cells can accelerate the restoration of the blood flow to the ischemic limb (Kalka et al., 2000; Schatteman et al., 2000).

In these studies, transdifferentiation or reprogramming has been substantiated mostly by cell morphology and/or the expression of antigenic proteins specific to the transplanted tissue. Few of these reports demonstrated new or restored functional responses. Here, we investigated whether epidermal

progenitor cells (EpPCs) could adopt a novel fate in phenotype and acquire a functional phenotype thus far undescribed from them. Our rationale was that, because epidermal cells are readily accessible and expandable, they could be valuable for cell-based therapy of local or systemic disorders.

Materials and Methods

Isolation and labeling of mouse epidermal cells

Epidermal cells were obtained from 1-day-old C57Bl/6 mice as previously described (Hager et al., 1999). Total basal keratinocytes were incubated in Hoechst 33342 ($2.5 \mu\text{g ml}^{-1}$) for 90 minutes at 37°C [with or without 50 mM Verapamil (Sigma, St Louis, MO)], resuspended in propidium iodide ($0.5 \mu\text{g ml}^{-1}$) and separated into progenitor and TA cells using a Becton Dickinson FACSDiVa cell sorter using the following arrangement. Forward and side scatter signals were produced using 150 mW at 488 nm from a Coherent 90C-4 argon ion laser. 100 mW of multi-line ultraviolet light from a Coherent 302C krypton laser was used for Hoechst and propidium-iodide excitation. Subsequent blue (424/44 BP filter) and red (675/20 BP filter) emissions were split using a 610 SP dichroic filter. Total unsorted epidermal cells are shown in a two-parameter plot of forward scatter (FSC-A) versus side scatter (SSC-A) in Fig. 1A. An initial amorphous gate was drawn in the plot to avoid debris (data not shown). Cells satisfying the first gate were passed to a second plot of forward versus side scatter in which another amorphous gate was drawn on the population representing the lowest 25% (P2 in Fig. 1A). Once these two gates were satisfied, progenitor cells were identified as those having low blue and red Hoechst content and that were verapamil sensitive (EpPC in Fig. 1C and D). TA cells were obtained by selecting the cells not designated as P2 in Fig. 1A. These cells were plotted according to their Hoechst blue and red fluorescence (Fig. 1B). No further gating was necessary for their isolation (Fig. 1B). Some sorted cells were cultured as previously described (Hager et al., 1999), whereas others were used fresh. Before injection, freshly isolated or cultured cells were labeled with CM-DiI (chloromethyl-1'-dioctadecyl-3,3,3',3'-tetramethylindocarbocyanine perchlorate; Molecular Probes, Eugene, OR), a red fluorescent dye that intercalates into cell membranes. Briefly, sorted cells were resuspended at 1×10^6 cells ml^{-1} and incubated in $5 \mu\text{g ml}^{-1}$ CM-DiI in N medium (Hager et al., 1999) for 10 minutes at 37°C , 15 minutes at 4°C and 2 hours at 37°C . Almost all the cells incorporated the dye ($98.9 \pm 0.4\%$ of EpPCs and $99.5 \pm 0.2\%$ of TA cells; $n=3$ for each group). Cells were pelleted and washed once with PBS before use to remove unincorporated dye.

Induction of diabetes and hindlimb ischemia

C57Bl/6 mice (Harlan, Indianapolis, IN) at 8-12 weeks of age were treated daily for 5 days with 40 mg kg^{-1} streptozotocin intraperitoneally (i.p.) (Sigma, St Louis, MO), a protocol that reduces the acute effects of streptozotocin (Kunjathoor et al., 1996). Glucose levels, which are typically stable for 7 weeks (Kunjathoor et al., 1996), were measured using Accu-Check glucometer (Roche, Indianapolis, IN) the following week as previously described and ranged from 187 mg ml^{-1} to 404 mg ml^{-1} . Mean glucose levels were similar between the groups (TA group, 276 ± 61 ; progenitor group, 268 ± 52 ; control, 325 ± 70 ; mean \pm s.d.). Except for a gradual weight loss, the health of the mice was not overtly affected by the treatment throughout the experimental period. Surgical induction of unilateral hindlimb ischemia was performed 3 weeks after diabetes induction, as described previously (Schatteman et al., 2000). The same surgery was also performed on non-diabetic 8-12-week-old C57Bl/6 mice. 3-5 hours after surgery, the ischemic limb was injected intramuscularly with freshly isolated (5×10^5 cells leg^{-1} in a total volume of $25 \mu\text{l}$) or cultured (1×10^5 cells leg^{-1} in a total volume of $25 \mu\text{l}$) CM-DiI-labeled progenitor cells, TA

cells, unsorted epidermal cells or dermal fibroblasts (as controls). Uninjected mice served as additional controls. All surgery was performed according to the University of Iowa Animal Care and Use Committee guidelines.

Two mice, each of which had each received 5×10^5 CM-DiI-labeled progenitor or TA cells were anesthetized 2 months later as described below and a PE10 catheter was introduced into the abdominal aorta. After anchoring the catheter, the vessel was anterogradely perfused with $200 \mu\text{g}$ of FITC-labeled *Bandeira simplicifolia* lectin B4 (F-BSLB₄, Vector Laboratories, Burlingame, CA) in $400 \mu\text{l}$ of 0.9% NaCl. 5 minutes later, the hindlimbs were perfused with 3-5 ml PBS, then with 3-5 ml of 4% paraformaldehyde. The muscle and overlying skin from the ischemic limb and contralateral limb muscle were harvested and post-fixed for 4 hours in 2% paraformaldehyde.

Blood-flow analysis

Laser Doppler imaging was used to assess blood flow in mouse hindlimbs (Couffinhal et al., 1998; Schatteman et al., 2000). Mice were anesthetized with ketamine ($91 \mu\text{g g}^{-1}$ i.p.) plus xylazine ($10 \mu\text{g g}^{-1}$ i.p.) and placed in the supine position. The hindlimbs were gently immobilized and scanned using a laser Doppler imager (Moor Instruments, Wilmington, DE), which measures the flux (blood cells per unit area per unit time) of blood. Scans were performed before the surgery (to verify that the flow was similar in the two limbs), immediately after the surgery (to verify that the operated limb was ischemic) and every other day for 12 days (to monitor the recovery of the blood flow). For each time point, between three and five scans were recorded. For analysis, equivalent areas ($\pm 5\%$) of the control and ischemic limbs from the same anatomical region of the limbs were compared. Mean flux in the selected areas was computed using the instrument's imaging software. Data are presented as the mean blood flux in the operated ischemic limb relative to flux in the unoperated control limb. Only mice in which the mean flux in the operated limb immediately after surgery was $<15\%$ that of the unoperated control limb were analysed. Potential divergence in flow over time curves was analysed using linear-regression analysis. The homogeneity of the variance was verified (Levene's statistic) then a one-way analysis of variance (Anova) followed by Bonferroni's post hoc analysis was used to compare data at specific time points. $P < 0.05$ was considered to be statistically significant.

Tissue preparation, cell preparation and immunolabeling

Muscle and skin above the injected muscle were collected from both hindlimbs. The liver was also collected. Tissues were fixed in 100% methanol, embedded in paraffin and sectioned at $7 \mu\text{m}$. Slides of sorted cells were prepared by spreading cells on microscope slides, drying and fixing in methanol/acetone 70/30 v/v at -20°C for 10 minutes. Immunostaining was performed as previously described (Michel et al., 1996) with minor modifications. Primary antibodies were rabbit anti-mouse keratin 14 (1/5000; Babco, Richmond, CA), rat anti-mouse CD31 (1/200-1/1000; Pharmingen, San Diego, CA), rabbit anti-mouse laminin (1/200; Chemicon, Temecula, CA), rat anti-mouse CD45 (Leukocyte common antigen, Ly-5; 1/100; Pharmingen) and rat anti-mouse Sca-1 (Ly-6A/E; 1/200; Pharmingen). Secondary antibodies were anti-rat FITC (1/100; Jackson Laboratories, West Grove, PA) and anti-rabbit Cy5 (1/100; Jackson Laboratories). Nuclear DNA was labeled with DAPI (Sigma) at the end of the staining procedure for 5 minutes at room temperature. An unmasking procedure [proteinase K (Roche), $10 \mu\text{g ml}^{-1}$ for 3 minutes at 37°C] was used before staining for CD31. Sections were mounted with Prolong[®] (Molecular Probes, Eugene, OR) and observed under a Nikon Eclipse 800 mounted with a RT-slider Spot digital camera. Images were taken in black and white, and pseudocolored. Three independent fields and a total of 1000 cells in at least two separate experiments were counted, and the proportion of positive cells

calculated as the number of positive cells divided by the total number of cells as determined by DAPI staining.

Capillary density

Lower hindlimb muscle from cell-treated and untreated limbs were harvested 14 days after induction of ischemia, then fixed in methanol and embedded in paraffin. Muscles were oriented for sectioning transverse to the limb and 200-250 serial 7 μm sections were mounted, beginning at the most distal end of the tibialis anterior and proceeding caudally. After rehydration, every 20th section was incubated for 1 hour with 5 μg ml⁻¹ biotinylated BSLB₄ (Vector Laboratories, Burlingame, CA), washed three times in PBS, incubated with Vector Red (Vector Laboratories) to visualize blood vessels and stained with hematoxylin (Coffin et al., 1991). Adjacent sections were stained with hematoxylin and eosin, and examined for overall morphology.

To determine the capillary-to-fiber ratios, the labeled sections were photographed at 400x. From the pictures, the number of muscle fibers and BSLB₄-labeled vessels were counted in two distinct regions. The first region contained healthy muscle (as judged by closely abutting fibers, lack of inflammatory infiltrate and peripheral nuclei) and the second lacked significant inflammatory infiltrate or necrotic cells and was undergoing muscle repair (as shown by muscle with central nuclei and dividing cells). Capillary analysis was not performed in necrotic regions or regions of muscle with extensive inflammatory infiltrate.

Confocal microscopy

Tissue injected with F-BSLB₄ was embedded in 2% agarose and

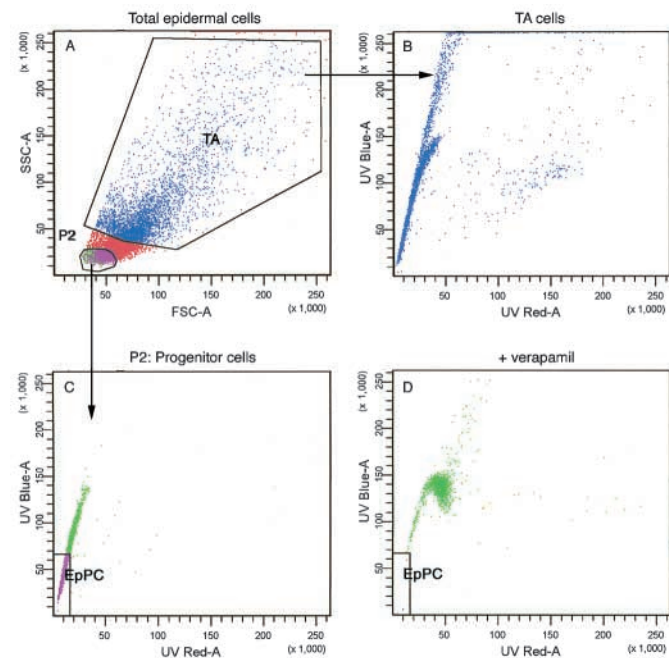


Fig. 1. FACS analysis of mouse epidermal cells sorted into progenitor and TA cells. The figure shows gates for EpPCs and TA cells as described in Materials and Methods.

vibrotome sections (200 μm) of mouse tissue were examined using a Bio-Rad 1024 confocal microscope (Bio-Rad, Hercules, CA). Both the rhodamine and fluorescein filters were used for each image collected during the scanning process. The z series was then converted into 32 projected images calculated from the original images throughout 53° of rotation about the x and y axes. Individual projected images at each point of rotation were captured and two animated movies of the projected images revolving through a 53° arc were subsequently created.

Results

Characterization of the sorted progenitor and TA cells

Epidermal cells were sorted into two distinct populations according to their forward scatter and their Hoechst red and blue content (Fig. 1). In order to characterize the progenitor and TA cells more precisely, we labeled the two cell populations with different antibodies. Our results (Table 1) show that about 90% of both cell populations were positive for keratin 14, indicating their keratinocyte phenotype. Both cell types were negative for CD31 (which labels endothelial cells) and Sca-1 [a marker of mouse hematopoietic stem cells (Ma et al., 2002; Morel et al., 1998)], whereas 0.9% and 0.2% of the TA and progenitor cells were positive for CD45 (marker for all cells of the blood lineage), respectively (Table 1).

Freshly isolated epidermal cells incorporate into the vasculature and change their phenotype

To determine the fate of freshly isolated epidermal cells injected into ischemic hindlimbs, we examined biopsies of muscle tissues taken 2 weeks and 5 weeks after the surgery. CM-DiI red-fluorescent cells were present in progenitor- and TA-cell-injected limbs, predominantly in the ischemic leg and rarely in the control leg. Similar results were observed in diabetic and non-diabetic animals. Labeled cells were found between muscle fibers, in connective tissue and in vascular-like structures. To determine whether the injected labeled cells were incorporated into the vasculature and differentiated, we performed immunostaining for CD31 and laminin. Laminin is a component of the endothelial cell basement membrane and presents on the abluminal side of endothelial cells. We found red, CM-DiI-labeled cells outside and inside the area delineated by the laminin (data not shown). We also used a CD31 antibody, which was detected using an FITC-tagged (green fluorescent) secondary antibody. Many red fluorescent and some CM-DiI anti-CD31 co-labeled (yellow) cells were found in the vessels (Fig. 2A-D). This suggests that some epidermal cells changed their phenotype, because CD31 was not expressed by the progenitor and TA cells before injection [Table 1; Fig. 2A, in which the epidermis (arrowheads) is labeled with keratin 14 (blue) only, and not CD31 (green)]. To evaluate whether the epidermal cells completely or partially lost their original characteristics, we performed double-

Table 1. Phenotypic characterization of sorted mouse epidermal cells

	Keratin 14	Pecam 1	Sca-1	CD45
EpPC	92.6±2.9*	0.005±0.01	0.05±0.04	0.203±0.2
TA	89.6±3.61	0.14±0.13	0.0675±0.02	0.89±0.86

*Values are means expressed in percentage of total cells±s.e.m.

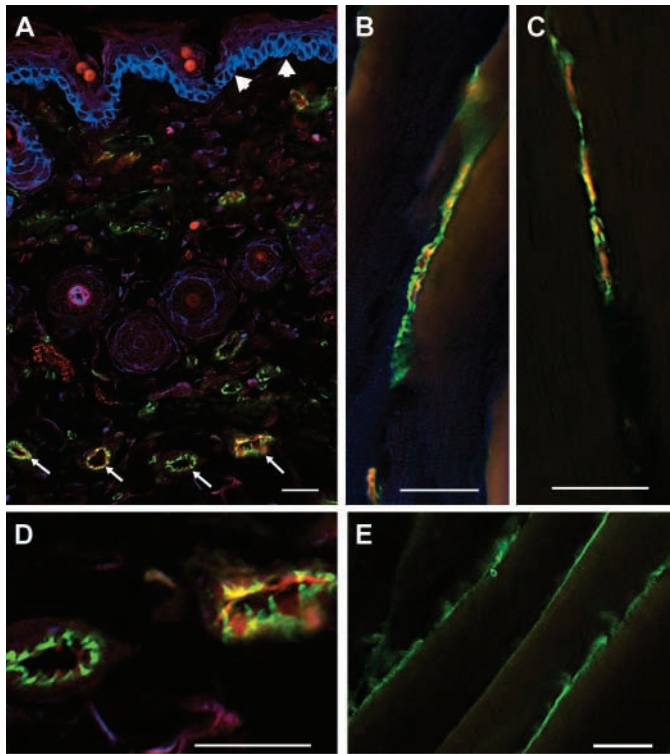


Fig. 2. Incorporation of freshly isolated epidermal cells into the vasculature. Freshly isolated epidermal progenitor cells (A,B) and transient amplifying cells (C) were labeled with CM-DiI (red fluorescent dye) and injected into a mouse ischemic hindlimb. Two weeks later, biopsies of skin (A,D) and ischemic muscles (B,C,E) were immunostained for CD31 (to identify endothelial cells; green) and keratin 14 (blue, a marker for epidermal basal cells; A, arrowheads). CM-DiI-labeled (red) cells, co-labeled CM-DiI and anti-CD31 (yellow) cells, but not keratin-14-positive (blue) cells can be seen in the vessels. Arrows indicate two capillaries enlarged in (D). No injected cells (red) could be seen in the vasculature (green) in the contralateral control muscle (E). Notice that the two red dots in (A) correspond to autofluorescent hair shaft cut in oblique sections and are not CM-DiI-injected cells. Scale bars, 25 μ m.

labeling immunofluorescence with CD31 and keratin 14, a marker for basal epidermal cells expressed by progenitor and TA cells (our study) (Fuchs and Green, 1980). As shown in Fig. 2A, keratin 14 (blue) was detected in the basal layer of the epidermis (arrowheads). However, keratin 14 was not detected in the CM-DiI-labeled cells (red or yellow when co-expressing CD31) in the vasculature of skin or muscle (Fig. 2A-D). Taken together, these findings suggest that a subset of epidermal cells incorporated into the endothelium, and responded to their new microenvironment by changing from an epithelial cell to an endothelial-cell-like phenotype.

To assess whether the injected epidermal cells remained in the muscles, we examined sections of liver and skin above the injected muscle. CM-DiI labeled progenitor and TA cells were found incorporated into the vessels of the dermis in the ischemic leg (Fig. 2A,D). However, the rare cells found in the control leg were never incorporated into vessel structures (Fig. 2E). Occasionally red-fluorescent cells were detected in liver of progenitor- but not TA-cell-injected mice (data not shown).

Because a two-dimensional image does not unambiguously

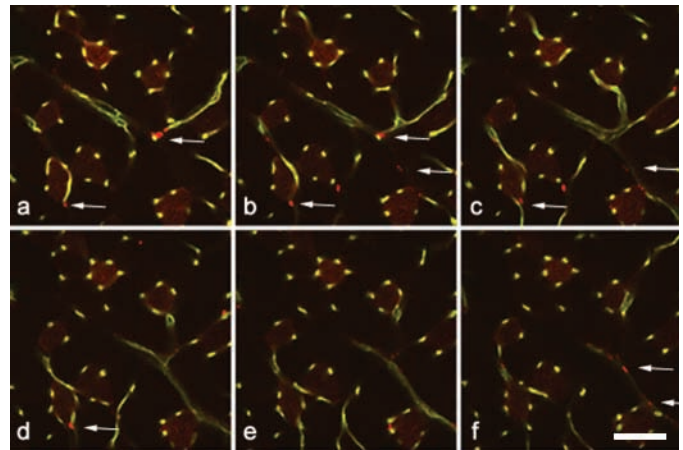


Fig. 3. Confocal images of epidermal cells incorporating into the vasculature. Epidermal cells were isolated, labeled with the red fluorescent dye CM-DiI and injected into diabetic mice with an ischemic leg. One month after the injection, mice were perfused with FITC-tagged BSLB₄ (a labelled lectin specific for mouse endothelial cells) before tissue was harvested. Pictures were taken with a confocal microscope. For this particular example, a z series of 60 focal plans was acquired 1.5 μ m apart. (a-f) Consecutive stacks of six images each. Notice the red fluorescent cells (epidermal cells labeled with CM-DiI, arrows) incorporated into the vasculature delineated by the green fluorescence. Scale bars, 25 μ m.

demonstrate incorporation into the vasculature, we performed three-dimensional reconstructions of confocal images after F-BSLB₄ perfusion. Some injected cells appeared to be incorporated into the vessel wall in the ischemic muscle (Fig. 3, arrows). By digitally rotating the three-dimensional reconstruction, we were able to distinguish cells that were in the vessel wall from those that were only near it. Many CM-DiI-labeled cells were found within the vessel wall [see Movie (<http://jcs.biologists.org/supplemental/>)].

Cultured epidermal progenitor and TA cells maintain the ability to incorporate into the neovasculature

In order to assess whether cells grown in culture could be detected in the vasculature, we plated epidermal progenitor and TA cells on collagen-IV-coated dishes and subcultured them twice. Cells were then CM-DiI labeled and injected into ischemic limbs. As with freshly isolated cells, we were able to detect CM-DiI-labeled cells in CD31-positive vessels of muscle (Fig. 4A,B). These results strongly suggest that cultured epidermal progenitor and TA cells, like freshly isolated epidermal cells, incorporated into the vasculature after being cultured *in vitro*, and some of them responded to their new environment and adopted an endothelial-cell-like phenotype.

Epidermal cells increase the restoration of the blood flow in diabetic ischemic limbs

To determine whether the injected sorted or unsorted epidermal cells could exert functions not yet described for skin cells, we tested their ability to accelerate the restoration of the blood flow to ischemic tissue of mice *in vivo*. We initially choose to

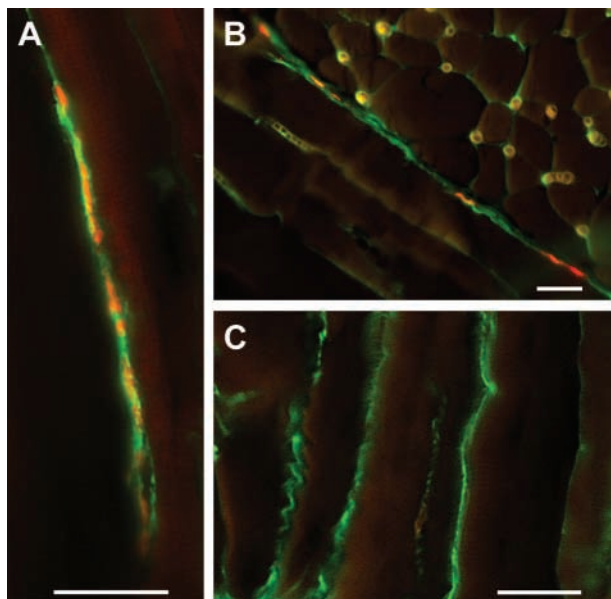


Fig. 4. Incorporation of cultured epidermal cells into the vasculature. Cultured epidermal progenitor cells (B) and transient amplifying cells (A) were labeled with CM-DiI (red fluorescent dye) and injected into a mouse ischemic hindlimb. Five weeks later, biopsies of ischemic muscles were immunostained for CD31 (to identify endothelial cells; green). CM-DiI-labeled (red) cells, co-labeled CM-DiI and anti-CD31 (yellow) cells can be seen in the vessels. No injected cells (red) could be seen in the vasculature (green) in the contralateral control muscle (C). Scale bars, 25 μ m.

work with diabetic animals because (i) their rate of neovascularization is lower than that of normal animals and (ii) the injection of blood-derived angioblasts accelerated blood-flow restoration in diabetic nude mice, whereas it had no effect on non-diabetic animals (Schatteman et al., 2000). Ischemia was surgically induced in the left hindlimb of adult diabetic C57Bl/6 mice. In this well-characterized model, the ligation of the femoral artery and the transection of the collateral vessels led to markedly reduced blood flow in the operated leg as assessed by laser Doppler imaging immediately after the surgery (Fig. 5) (Couffinhil et al., 1998).

Hindlimb blood flow was measured using laser Doppler

imaging before, immediately after and every other day after surgery to assess the restoration of blood flow to the ischemic limb. When fibroblasts or no cells were injected into the muscle (control animals), the blood flow was restored to only 32% and 33% of its normal level 12 days after the surgery, respectively (Fig. 6). However, the injection of EpPCs significantly accelerated the recovery of the blood flow. This trend was apparent by 8 days, when the blood flow was 39% of its normal level (Figs 5, 6) and was statistically significant ($P < 0.05$) at day 10 (44%) and day 12 (55%). By contrast, although TA cells incorporated into the vasculature, they did not appear to affect the restoration of the blood flow significantly (Fig. 6). Interestingly, the presence of unsorted cells in the ischemic limb accelerated the restoration of the blood flow and their effect was more profound than the TA or EpPCs alone. Later time points were not recorded because the health of diabetic animals typically begins to deteriorate beginning about 14 days after surgery.

Capillary density and muscle morphology

To determine whether the increased blood flow correlated with muscle salvage and higher capillary density, distal hindlimb muscle was examined for morphology and vascularization 14 days after induction of ischemia. Histological examination revealed four distinct muscle morphologies: (1) healthy muscle with peripheral nuclei and tightly abutted fibers (Fig. 7A); (2) successfully regenerating muscle with little inflammatory infiltrate but central nuclei and many dividing cells (Fig. 7B); (3) marginally regenerating muscle, characterized by moderate to extensive inflammatory infiltrate, occasional necrotic cells, central nuclei and some dividing cells (Fig. 7C); and (4) necrotic muscle (Fig. 7D). All mice had similar amounts of healthy muscle, essentially all of which was composed of large-diameter fibers. However, although necrotic areas were extensive in untreated and fibroblast-treated limbs, necrotic regions were not common in TA-cell or EpPC-treated limbs. Instead large areas of regenerating or marginally regenerating muscle were present in these groups.

Capillary-per-fiber ratios were determined in healthy and successfully regenerating muscle and did not differ among cell-treated groups. Ratios for EpPC-, TA-cell- and fibroblast-treated muscle were 0.91 ± 0.02 , 1.04 ± 0.07 and 0.96 ± 0.02 in healthy muscle, and 1.84 ± 0.23 , 1.97 ± 0.31 and 1.97 ± 0.29 in

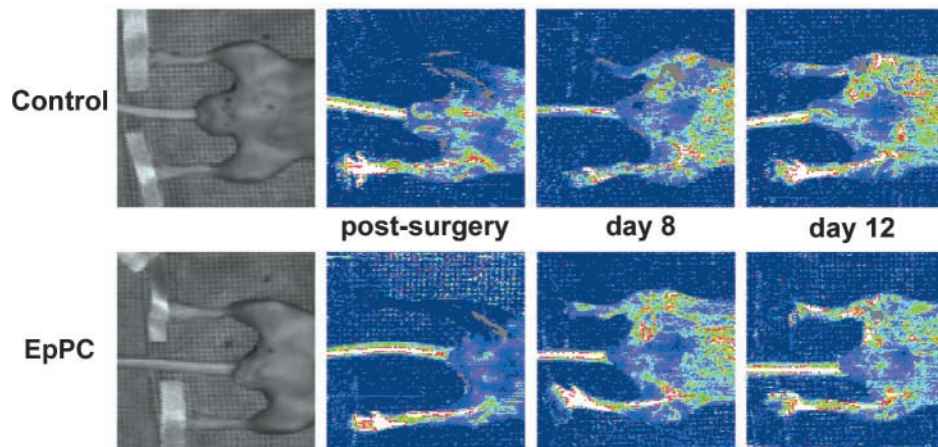


Fig. 5. Laser Doppler blood-flow images. Representative images of control (buffer or fibroblast injected) and diabetic animals injected with EpPCs. Mice were monitored before the surgery to verify the integrity of the blood flow and every other day after the surgery to evaluate the restoration of the blood flow. Dark blue areas represent area with no flow and white areas represent regions with the highest flow. Notice the lack of flow immediately after the surgery. After 12 days, the flux was restored to 33% in the control buffer-injected animals, compared with 55% in the progenitor-cell-injected animals.

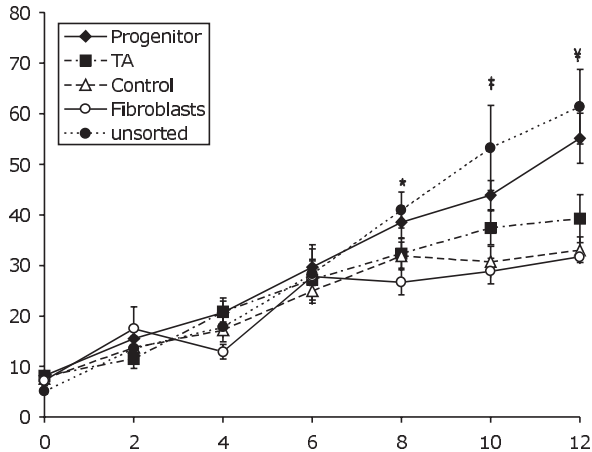


Fig. 6. Restoration of the blood flow in surgically induced ischemia in diabetic mouse hindlimbs. The data are expressed as the percentage of blood flow in the operated limb relative to the contralateral unoperated limb from the same animal. Fluxes were measured using a scanning laser Doppler and means of between three and five readings were calculated for each animal at each time point. Averages of means for 4–16 animals were plotted as a function of time. Error bars represent standard error. *, Unsorted cells significantly different to fibroblast-injected and control animals by one-way Anova ($P < 0.05$); ‡, unsorted and progenitor cells significantly different to fibroblast-injected and control animals by one-way Anova ($P < 0.05$); ¥, unsorted cells, progenitor cells and TA cells significantly different from fibroblast-injected and control animals by one-way Anova ($P < 0.05$). The linear regression of the flow from progenitor-cell-injected animals was also significantly different from the control animals by one-way Anova ($P < 0.05$).

regenerating muscle, respectively. Ratios were not determined in marginally regenerating muscle, in which the extensive inflammatory infiltrate made it difficult to obtain accurate counts, nor in necrotic regions, in which ratios varied as much as tenfold in different areas of a single tissue section.

Epidermal TA cells affect the restoration of the blood flow in non-diabetic animals

Injection of blood-derived endothelial-cell progenitors accelerated blood-flow restoration in diabetic nude mice and not in non-diabetic animals (Schatteman et al., 2000), but a related subset of blood-derived cells improved flow in non-diabetic C57Bl/6 mice (Kalka et al., 2000). Hence, we tested the effects of epidermal cells in non-diabetic mice as well. As with diabetic animals, we measured hindlimb blood flow using laser Doppler imaging before, immediately after and every other day after surgery in control, EpPC- and TA-cell-injected mice (Fig. 8). Injection of epidermal cells rapidly accelerated the recovery of the blood flow compared with the control. A profound TA-cell-mediated increase in flow relative to controls was apparent by 2 and 4 days ($P < 0.05$). EpPCs exhibited a similar trend but the effect was not significant until day 8. Because there was variability in the epidermal cell data ($n = 5$ in each group) but the trends were similar for both TA and EpPCs, we also analysed the data by grouping EpPCs and TA cells together as epidermal cells ($n = 10$). As a group, the epidermal cells significantly accelerated the restoration of flow

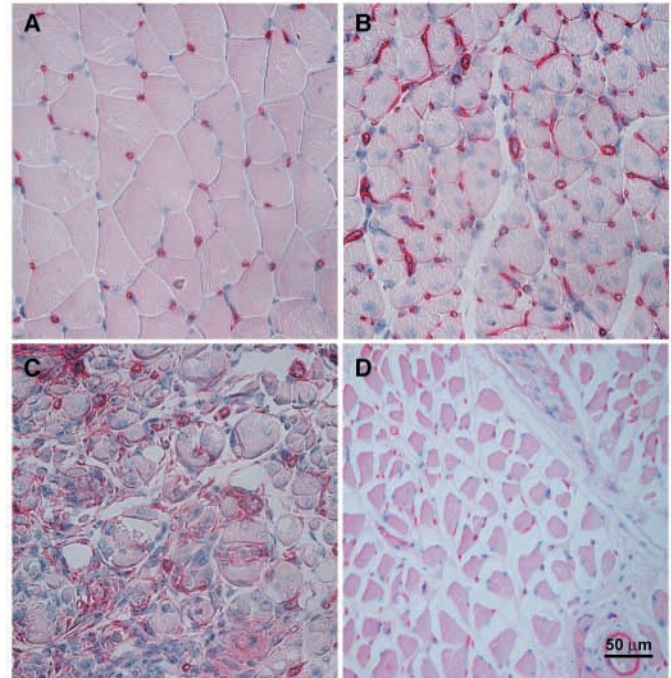


Fig. 7. Histology and vascularization of muscle in ischemic hindlimbs 14 days after iliac artery ligation. Hematoxylin and eosin stained 7 µm transverse sections of muscle in the lower hindlimb at the level of the distal gastrocnemius muscle. Sections were incubated with BSLB₄ and reacted with Vector Red to visualize blood vessels (bright red). (A–C) A limb treated with progenitor cells. (D) A fibroblast-treated limb. (A) Healthy muscle. (B) Recovering muscle. (C) Severely injured recovering muscle with inflammatory infiltrate. (D) Necrotic muscle. Scale bar, 50 µm.

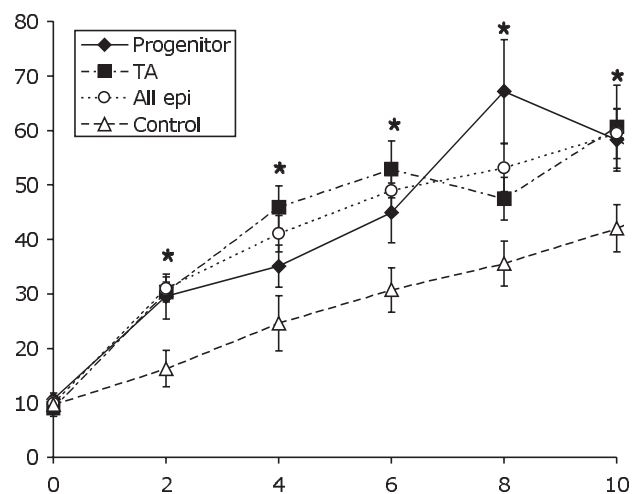


Fig. 8. Restoration of the blood flow in surgically induced ischemia in non-diabetic mouse hindlimbs. The data are expressed as the percentage of blood flow in the operated limb relative to the contralateral unoperated hindlimb from the same animal. Fluxes were measured using a scanning laser Doppler and means of between three and five readings were calculated for each animal at each time point. Averages of means for 5–11 animals were plotted as a function of time. Error bars represent standard error. *, Statistically significant difference from the control animals by one-way Anova ($P < 0.05$) at days 2–6 for the TA group, and at days 8–10 for the progenitor group.

relative to uninjected controls on days 2-10 after induction of ischemia. By day 12, flow in untreated limbs begins to catch up to that of treated limbs and blood-flow restoration was not significantly different between the two groups. The flow restoration appears to persist, at least in epidermal-cell-treated mice, because flow restoration was $66.6 \pm 2.5\%$ ($n=2$) and $69.9 \pm 1.2\%$ ($n=2$) of the control limb at 3 months for EpPC- and TA-cell-treated mice, respectively. Overall, the level of restoration of the blood flow was higher in the non-diabetic than the diabetic animals (Figs 6, 8).

Discussion

Many reports have been published recently concerning adult stem cells and their plasticity. Typically, these studies describe phenotypic switches from cell types of the stem-cell tissue of origin to antigenic phenotypes characteristic of cells from different tissues. Among these studies, few demonstrated that the donor-derived cells acquired new functions thus far unknown to them. Only two reports focused on skin (Liang and Bickenbach, 2002; Toma et al., 2001). One of the reasons for the rarity of studies on epidermal stem cells is the lack of specific markers and the difficulties isolating these cells. As described here, we optimized a method that allows us to obtain an enriched population of mouse EpPCs, giving us the opportunity to address basic questions about their biology, fate and, in this report, plasticity.

To test our hypothesis that EpPCs, like many other progenitor cells in the adult, are pluripotent, we used a well-established diabetic mouse ischemic hindlimb model. In this model, ischemia is created by surgical ligation of the femoral artery and collateral vessels following induction of diabetes with streptozocin treatment. Neovascularization occurs rapidly, although more slowly in diabetic than in non-diabetic animals, and the histological sequence of neovascularization corresponds temporally to blood-flow recovery as measured by laser Doppler analysis (Couffinhal et al., 1998). This model has been used primarily to evaluate the effect of growth factors on neovascularization (Couffinhal et al., 1998; Taniyama et al., 2001) but, more recently, it was used to help elucidate which cell types contribute to the formation of new blood vessels. For example, bone-marrow transplantation was performed in combination with the induction of ischemia and donor cells were found in neovessels (Asahara et al., 1999). In other experiments, CD34⁺ hematopoietic cells accelerated the restoration of the blood flow in diabetic mice (Schatteman et al., 2000).

We asked whether EpPCs incorporate into the vasculature after induction of ischemia, and the answer appears to be yes. We detected injected CM-Dil-labeled epidermal cells in the endothelium of capillaries 2 and 5 weeks after injection. Not only EpPCs but also TA cells (or the daughter cells of the progenitor cells) were incorporated into the vasculature. In accordance with the recent findings that adult stem cells from various tissues are multipotent (Krause et al., 2001; Orlic et al., 2001; Theise et al., 2000b) (for review, see Blau et al., 2001), our results suggest that EpPCs share the same property. The detection of TA cells in the endothelium was somewhat more surprising, although TA cells from the cornea can be reprogrammed under the influence of embryonic dermis (Ferraris et al., 2000) and epidermal murine TA cells are

capable of recapitulating an epidermis *in vitro* (Dunnwald et al., 2001). Localized in the basal layer of the epidermis, TA cells proliferate for a finite period of time before terminally differentiating. Thus, these cells exhibit characteristics of more differentiated cells. Interestingly, monocytes (differentiated progenitors of dendritic cells and macrophages) can also differentiate into endothelial cells (Fernandez-Pujol et al., 2001; Harraz et al., 2001). Our previous studies showed that, although both EpPCs and TA cells grew in culture, could be transduced and recapitulated an epidermis on the top of a bioengineered dermis, only the EpPCs survived in the long term (Dunnwald et al., 2001). Therefore, it is possible that TA cells are lost from the vessel wall later than our biopsies at 5 weeks.

As with other types of progenitor cell, EpPCs accelerated the restoration of blood flow to the ischemic limbs in diabetic mice ($44 \pm 3\%$ vs $29 \pm 2\%$ at day 10; $55 \pm 5\%$ vs $32 \pm 1\%$ at day 12) but the presence of TA cells in the vasculature of diabetic animals did not. This demonstrates that incorporation of the cells alone is not sufficient to accelerate the restoration of blood flow but rather that acceleration of flow requires a second function to be present.

In contrast to diabetic animals, a significant TA cell-mediated increase in flow relative to controls and a progenitor-induced trend towards improvement were apparent by 2 days in non-diabetic animals. This increase was maintained by EpPCs or TA cells through day 10. From the data, one might conclude that TA cells exert their effects on flow more rapidly than do progenitors, although (because of variability in the data) both cell types might have similar effects on flow restoration in a non-diabetic environment. However, in the diabetic environment, progenitor-mediated improvements in flow were not suggested until day 8 and were not significant until day 10. It is worth investigating this point further because it could have important clinical applications, especially when an immediate effect is required. TA cells are more numerous and a larger proportion of them are actively dividing compared with EpPCs (Tani et al., 2000). Therefore, TA cells could be a more attractive therapeutic candidate than progenitor cells in some cases.

We have previously shown that blood-derived EpPC function is impaired by diabetes and that non-diabetic progenitor cells function differently in diabetic than non-diabetic environments (Harraz et al., 2001; Schatteman et al., 2000; Stepanovic et al., 2003). Similarly, in this study, the effects of TA cells were different in the diabetic and non-diabetic environments, suggesting that TA cells might need co-factors to exert their effects and that these factors are absent or downregulated in the diabetic mice. Indeed, in the hematopoietic system, co-injection of CD34⁺ progenitor cells (analogous to EpPCs) with putative CD14⁺ endothelial cell precursors (analogous to TA cells) appears to induce the incorporation of the endothelial cell precursors into the vasculature (Harraz et al., 2001). Perhaps co-injection of TA cells with progenitor cells would have additive effects such that restoration of the blood flow would be greater than that induced by progenitor cells alone. In support of our hypothesis, our data indicate that injection of total unsorted epidermal cells (which include the progenitor and the TA cells, as well as more differentiated cells) into diabetic mice profoundly accelerates flow restoration. This is consistent with the idea that progenitor

cells are maintained as such by their neighboring progeny and that cell-cell interactions play a crucial role in determining cellular phenotype. This theory of the 'niche' has been reported in many tissues and organisms, including the bulge area of the hair follicle in the skin (Lavker and Sun, 2000; Nishimura et al., 2002), the bottom of the crypt in the gut epithelium (Potten and Morris, 1988), the limbus of the eye (Cotsarelis et al., 1989), the *Drosophila* ovary (Song et al., 2002; Xie and Spradling, 2000) and the middle of the shoot meristem in *Arabidopsis* (Mayer et al., 1998).

Although capillary density and blood flow are not necessarily linked, we were surprised to find that histological analysis revealed no differences in capillary-to-fiber ratios in the healthy and successfully repairing portions of the ischemic limbs among mice from the various cell-treatment groups. However, whereas extensive repairing and little necrotic muscle were found in epidermal-cell-treated animals, the reverse was true in fibroblast-treated limbs. Because high capillary density is associated with successfully repairing tissue, overall limb capillary density was probably higher in epidermal-cell-treated than fibroblast-treated limbs, and it is possible that a difference in capillary density might have been apparent had limbs been examined at earlier time points. Nevertheless, increased flow without increased capillary density would also result in improved muscle rescue. Therefore, whether improvements in tissue perfusion were due to increased flow, increased capillary density or both, the ultimate effect was limb muscle rescue.

Despite the fact that EpPCs incorporated into the endothelium and accelerated the restoration of blood flow after ischemia, their apparent level of incorporation into the vessels seems to be too low to account for the difference in the flow restoration. One explanation is that the injected cells proliferated rapidly, thereby diluting the loaded dye and rendering them undetectable. Another possibility is that the EpPCs actively recruit endogenous cells to form new blood vessels or to remodel existing ones. This could be achieved by epidermal cells producing chemoattractants for endothelial cells, which would then form the new vessels. Vascular endothelial growth factor has been shown to be produced at low levels by keratinocytes (Weninger et al., 1996) and could be induced in these cells *in vivo* by the ischemia. Another possibility is that the ischemic microenvironment induces the epidermal cells to modify their phenotype and function. As a consequence, as well as expressing endothelial cell markers, EpPCs would also secrete angiogenic proteins normally produced by endothelial cells (e.g. angiopoietin). Further investigations will be required to understand fully the underlying mechanisms that trigger EpPCs to acquire a new phenotype (endothelial cell phenotype) and to show new functional capabilities (acceleration of the blood flow).

In conclusion, we demonstrated that both EpPCs and TA cells can incorporate into the endothelium and enhance the restoration of the blood flow to ischemic hindlimbs, and that they might act synergistically to do so. Diabetes specifically impairs the ability of exogenous TA cells to enhance blood-flow restoration but co-injection with epidermal progenitors can overcome this functional impairment. Freshly isolated and cultured epidermal cells were detected as long as 5 weeks after a single injection, suggesting that these donor-derived cells survived long-term *in vivo*. As such, epidermal cells might

constitute a cell-based therapy for ischemia. Because the skin is so easy to access and epidermal cells can be expanded in culture, the epidermis constitutes a readily available source of plastic cells. These cells might be ideal candidates not only for cell-based therapy for ischemia but also for non-viral gene delivery in gene therapy and for the long-term delivery of proteins like insulin in diabetes.

We thank E. Lazartigues for help with statistical analysis and R. Davisson for critical reading of the manuscript. We also thank E. Gelman and A. Mattox for their technical help. Sorting epidermal progenitor and TA cells was performed at The University of Iowa Flow Cytometry Core Facility (J. Fishbaugh and G. Hess). This work was supported by NIH/NIDDK grants (Gene Therapy Center grant) P30 DK54759 (M.D.) and DK59223 and DK55965 (G.S.). In addition, work was supported by the Juvenile Diabetes Research Foundation grant 1-2001-534 (G.S.) and a departmental endowment from the Herzog Foundation and the generous support of the Joe Marshall Family of Morningside, Iowa (M.D.).

References

- Asahara, T., Murohara, T., Sullivan, A., Silver, M., van der Zee, R., Li, T., Witzenbichler, B., Schattman, G. C. and Isner, J. M. (1997). Isolation of putative progenitor endothelial cell for angiogenesis. *Science* **275**, 964-967.
- Asahara, T., Masuda, H., Takahashi, T., Kalka, C., Pastore, C., Silver, M., Kearney, M., Magner, M. and Isner, J. M. (1999). Bone marrow origin of endothelial progenitor cells responsible for postnatal vasculogenesis in physiological and pathological neovascularization. *Circ. Res.* **85**, 221-228.
- Bickenbach, J. R. and Dunnwald, M. (2000). Epidermal stem cells: characteristics and use in tissue engineering and gene therapy. *Adv. Dermatol.* **16**, 159-184.
- Blau, H. M., Brazelton, T. R. and Weimann, J. M. (2001). The evolving concept of a stem cell: entity or function? *Cell* **105**, 829-841.
- Coffin, J. D., Harrison, J., Schwartz, S. and Heimark, R. (1991). Angioblast differentiation and morphogenesis of the vascular endothelium in the mouse embryo. *Dev. Biol.* **148**, 51-62.
- Cotsarelis, G., Cheng, S. Z., Dong, G., Sun, T.-T. and Lavker, R. M. (1989). Existence of slow-cycling limbal epithelial basal cells that can be preferentially stimulated to proliferate: implications on epithelial stem cells. *Cell* **57**, 201-209.
- Couffignal, T., Silver, M., Zheng, L. P., Kearney, M., Witzenbichler, B. and Isner, J. (1998). Mouse model of angiogenesis. *Am. J. Pathol.* **152**, 1667-1679.
- Dunnwald, M., Tomanek-Chalkey, A., Alexandrunas, D., Fishbaugh, J. and Bickenbach, J. R. (2001). Isolating a pure population of epidermal stem cells for use in tissue engineering. *Exp. Dermatol.* **10**, 45-54.
- Eglitis, M. A. and Mezey, E. (1997). Hematopoietic cells differentiate into both microglia and macroglia in the brains of adult mice. *Proc. Natl. Acad. Sci. USA* **94**, 4080-4085.
- Fernandez-Pujol, B., Lucibello, F. C., Zuzarte, M., Lutjens, P., Muller, R. and Havemann, K. (2001). Dendritic cells derived from peripheral monocytes express endothelial markers and in the presence of angiogenic growth factors differentiate into endothelial-like cells. *Eur. J. Cell Biol.* **80**, 99-110.
- Ferrari, G., Cusella-De Agelis, G., Coletta, M., Paolucci, E., Stornaiuolo, A., Cossu, G. and Mavilio, F. (1998). Muscle regeneration by bone marrow-derived myogenic progenitors. *Science* **279**, 1528-1530.
- Ferraris, C., Chevalier, G., Favier, B., Jahoda, C. A. B. and Dhouailly, D. (2000). Adult corneal epithelium basal cells possess the capacity to activate epidermal, pilosebaceous and sweat gland genetic programs in response to embryonic dermal stimuli. *Development* **127**, 5487-5495.
- Fuchs, E. and Green, H. (1980). Changes in keratin gene expression during terminal differentiation of the keratinocyte. *Cell* **19**, 1033-1042.
- Goodell, M. A., Brose, K., Paradis, G., Conner, A. S. and Mulligan, R. C. (1996). Isolation and functional properties of murine hematopoietic stem cells that are replicating *in vivo*. *J. Exp. Med.* **183**, 1797-1806.
- Gussoni, E., Soneoka, Y., Strickland, C. D., Buzney, E. A., Khan, M. K., Flint, A. F., Kunkel, L. M. and Mulligan, R. C. (1999). Dystrophin

- expression in the *mdx* mouse restored by stem cell transplantation. *Nature* **401**, 390-394.
- Hager, B., Bickenbach, J. R. and Fleckman, P. (1999). Long term culture of murine epidermal keratinocytes. *J. Invest. Dermatol.* **112**, 971-976.
- Hall, P. A. and Watt, F. M. (1989). Stem cells: the generation and maintenance of cellular diversity. *Development* **106**, 619-633.
- Harratz, M., Jiao, C., Hanlon, H. D., Hartley, R. S. and Schatteman, G. C. (2001). CD34⁺ expanded-derived human endothelial cell progenitors. *Stem Cells* **19**, 304-312.
- Jackson, K. A., Majka, S. M., Wang, H., Pocius, J., Hartley, C. J., Majesky, M. W., Entman, M. L., Michael, L. H., Hirschi, K. K. and Goodell, M. A. (2001). Regeneration of ischemic cardiac muscle and vascular endothelium by adult stem cells. *J. Clin. Invest.* **107**, 1395-1402.
- Kalka, C., Masuda, H., Takahashi, T., Kalka-Moll, W. M., Silver, M., Kearney, M., Li, T., Isner, J. M. and Asahara, T. (2000). Transplantation of ex vivo expanded endothelial progenitor cells for therapeutic neovascularization. *Proc. Natl. Acad. Sci. USA* **97**, 3422-3427.
- Kopen, G. C., Prockop, D. J. and Phinney, D. G. (1999). Marrow stromal cells migrate throughout forebrain and cerebellum, and they differentiate into astrocytes after injection into neonatal mouse brains. *Proc. Natl. Acad. Sci. USA* **96**, 10711-10716.
- Krause, D. S., Theise, N. D., Collector, M. I., Henegariu, O., Hwang, S., Gardner, R., Neutzel, S. and Sharkis, S. J. (2001). Multi-organ, multi-lineage engraftment by a single bone marrow-derived stem cell. *Cell* **105**, 369-377.
- Kunjathoor, V. V., Wilson, D. L. and LeBoeuf, R. C. (1996). Increased atherosclerosis in streptozocin-induced diabetic mice. *J. Clin. Invest.* **97**, 1767-1773.
- Lagasse, E., Connors, H., Al-Dhalimy, M., Reitsma, M., Dohse, M., Osborne, L., Wang, X., Finegold, M., Weissman, I. L. and Grompe, M. (2000). Purified hematopoietic stem cells can differentiate into hepatocytes in vivo. *Nat. Med.* **6**, 1229-1234.
- Lavker, R. M. and Sun, T.-T. (2000). Epidermal stem cells: properties, markers, and location. *Proc. Natl. Acad. Sci. USA* **97**, 13473-13475.
- Liang, L. and Bickenbach, J. R. (2002). Somatic epidermal stem cells can produce multiple cell lineages during development. *Stem Cells* **20**, 21-31.
- Ma, X., Robin, C., Ottersbach, K. and Dzierzak, E. (2002). The *Ly-6A (Sca-1)* GFP transgene is expressed in all adult mouse hematopoietic stem cells. *Stem Cells* **20**, 514-522.
- Mayer, K. F. X., Schoof, H., Haecker, A., Lenhard, M., Jurgens, G. and Laux, T. (1998). Role of *WUSCHEL* in regulating stem cell fate in the *Arabidopsis* shoot meristem. *Cell* **95**, 805-815.
- Mezey, E., Chandross, K. J., Harta, G., Maki, R. A. and McKercher, S. R. (2000). Turning blood into brain: cells bearing neuronal antigens generated in vivo from bone marrow. *Science* **290**, 1779-1782.
- Michel, M., Török, N., Godbout, M.-J., Lussier, M., Gaudreau, P., Roy, A. and Germain, L. (1996). Keratin 19 as a biochemical marker of skin stem cells in vivo and in vitro: keratin 19 expressing cells are differentially localized in function of anatomic sites, and their number varies with donor age and culture stage. *J. Cell. Sci.* **109**, 1017-1028.
- Morel, F., Galy, A., Chen, B. and Svilassy, S. J. (1998). Equal distribution of competitive long-term repopulating stem cells in the CD34⁺ and CD34⁻ fractions of *Thy-1* low *Lin*⁻low *Sca-1*⁺ bone marrow cells. *Exp. Hematol.* **26**, 440-448.
- Nishimura, E., Jordan, S. A., Oshima, H., Yoshida, H., Osawa, M., Moriyama, M., Jackson, I. J., Barrandon, Y., Miyachi, Y. and Nishikawa, S.-I. (2002). Dominant role of the niche in melanocyte stem-cell fate determination. *Nature* **416**, 854-860.
- Orlic, D., Kajstura, J., Chimenti, S., Jakoniuk, I., Anderson, S. M., Li, B., Pickel, J., McKay, R., Nadal-Ginard, B., Bodine, D. M. et al. (2001). Bone marrow cells regenerate infarcted myocardium. *Nature* **410**, 701-705.
- Oshima, H., Rochat, A., Kedzia, C., Kobayashi, K. and Barrandon, Y. (2001). Morphogenesis and renewal of hair follicles from adult multipotent stem cells. *Cell* **104**, 233-245.
- Petersen, B. E., Bowen, W. C., Patrene, K. D., Mars, W. M., Sullivan, A. K., Murase, N., Boggs, S. S., Greenberger, J. S. and Goff, J. P. (1999). Bone marrow as a potential source of hepatic oval cells. *Science* **284**, 1168-1170.
- Potten, C. S. and Morris, R. J. (1988). Epithelial stem cells in vivo. *J. Cell. Sci.* **10** (Suppl.), 45-62.
- Potten, C. S. and Loeffler, M. (1990). Stem cells: attributes, cycles, spirals, pitfalls and uncertainties. Lessons for and from the crypt. *Development* **110**, 1001-1020.
- Schatteman, G. C., Hanlon, H. D., Jiao, C., Dodds, S. G. and Christy, B. A. (2000). Blood-derived angioblasts accelerate blood-flow restoration in diabetic mice. *J. Clin. Invest.* **106**, 571-578.
- Song, X., Zhu, C.-H., Doan, C. and Xie, T. (2002). Germline stem cells anchored by adherens junctions in the *Drosophila* ovary niches. *Science* **296**, 1855-1857.
- Stepanovic, V., Awad, O., Jiao, C., Dunnwald, M. and Schatteman, G. C. (2003). Leprd diabetic mouse bone marrow cells inhibit skin wound vascularization but promote wound healing. *Circ. Res.* **92**, 1247-1253.
- Tani, H., Morris, R. J. and Kaur, P. (2000). Enrichment for murine keratinocyte stem cells based on cell surface phenotype. *Proc. Natl. Acad. Sci. USA* **97**, 10960-10965.
- Taniyama, Y., Morishita, R., Aoki, M., Nakagami, H., Yamamoto, K., Yamazaki, K., Matsumoto, K., Nakamura, T., Kaneda, Y. and Ogihara, T. (2001). Therapeutic angiogenesis induced by human hepatocyte growth factor gene in rat and rabbit hindlimb ischemia models: preclinical study for treatment of peripheral arterial disease. *Gene Ther.* **8**, 181-189.
- Taylor, G., Lehrer, M. S., Jensen, P. J., Sun, T.-T. and Lavker, R. M. (2000). Involvement of follicular stem cells in forming not only the follicle but also the epidermis. *Cell* **102**, 451-461.
- Theise, N. D., Badve, S., Saxena, R., Henegariu, O., Sell, S., Crawford, J. M. and Krause, D. S. (2000a). Derivation of hepatocytes from bone marrow cells in mice after radiation-induced myeloablation. *Hepatology* **31**, 235-240.
- Theise, N. D., Nimmakayalu, M., Gardner, R., Illei, P. B., Morgan, G., Teperman, L., Henegariu, O. and Krause, D. S. (2000b). Liver from bone marrow in humans. *Hepatology* **32**, 11-16.
- Toma, J. G., Akhavan, M., Fernandes, K. J. L., Barnabe-Heider, F., Sadikot, A., Kaplan, D. R. and Miller, F. D. (2001). Isolation of multipotent adult stem cells from the dermis of mammalian skin. *Nat. Cell Biol.* **3**, 778-784.
- Weninger, W., Uthman, A., Pammer, J., Pichler, A., Ballaun, C., Lang, I. M., Plettenberg, A., Bankl, H. C., Sturzl, M. and Tschachler, E. (1996). Vascular endothelial growth factor production in normal epidermis and in benign and malignant epithelial skin tumors. *Lab. Invest.* **75**, 647-657.
- Xie, T. and Spradling, A. C. (2000). A niche maintaining germ line stem cells in the *Drosophila* ovary. *Science* **290**, 328-330.